Research

New Phytologist

Nocturnal stomatal conductance in wheat is growth-stage specific and shows genotypic variation

Lorna McAusland[1], Kellie E. Smith[1], Alexander Williams[1], Gemma Molero[2] and Erik H. Murchie[1]

[1]School of Biosciences, University of Nottingham, Sutton Bonington, LE12 5RD, UK; [2]International Maize and Wheat Improvement Center (CIMMYT), Km. 45, Carretera Mexico, El Batan Texcoco, CP 56237, Mexico

Author for correspondence:
Lorna McAusland
Email: lorna.mcausland@nottingham.ac.uk

Received: *3 March 2021*
Accepted: *9 June 2021*

New Phytologist (2021) **232:** 162–175
doi: 10.1111/nph.17563

Key words: growth stage, nocturnal conductance, stomata, *Triticum aestivum*, water-use efficiency.

Summary

- Nocturnal stomatal conductance (g_{sn}) represents a significant source of water loss, with implications for metabolism, thermal regulation and water-use efficiency. With increasing nocturnal temperatures due to climate change, it is vital to identify and understand variation in the magnitude and responses of g_{sn} in major crops.
- We assessed interspecific variation in g_{sn} and daytime stomatal conductance (g_s) in a wild relative and modern spring wheat genotype. To investigate intraspecific variation, we grew six modern wheat genotypes and two landraces under well watered, simulated field conditions.
- For the diurnal data, higher g_{sn} in the wild relative was associated with significantly lower nocturnal respiration and higher daytime CO_2 assimilation while both species exhibited declines in g_{sn} post-dusk and pre-dawn. Lifetime g_{sn} achieved rates of 5.7–18.9% of g_s. Magnitude of g_{sn} was genotype specific 'and positively correlated with g_s. g_{sn} and g_s were significantly higher on the adaxial surface. No relationship was determined between harvest characteristics, stomatal morphology and g_{sn}, while cuticular conductance was genotype specific. Finally, for the majority of genotypes, g_{sn} declined with age.
- Here we present the discovery that variation in g_{sn} occurs across developmental, morphological and temporal scales in nonstressed wheat, presenting opportunities for exploiting intrinsic variation under heat or water stressed conditions.

Introduction

Plant responses to nocturnal environmental conditions are probably an under-represented field of plant ecophysiology. Nocturnal stomatal conductance (g_{sn}) describes the active opening of stomata at night and is independent of passive cuticular conductance (g_{min}), which is estimated to account for up to one-tenth the values observed for g_{sn} (Duursma *et al.*, 2019). Nocturnal stomatal behaviour is at first sight a conundrum; while daytime stomatal opening (g_s) balances the exchange of CO_2 for photosynthetic CO_2 assimilation (A) with water transpired, g_{sn} appears to maintain water loss with no carbon gain, reducing whole plant water-use efficiency and potentially increasing vulnerability to subsequent heat and drought stress (Howard *et al.*, 2009). In addition, g_{sn} may increase exposure to harmful pollutants such as ozone (Matyssek *et al.*, 1995). The responses of daytime g_s are well established (Lawson & Matthews, 2020); demonstrating closure in response to decreases in light, humidity and high CO_2, and opening in response to the inverse conditions. By contrast, g_{sn} responses have been species specific; demonstrating both positive (Caird *et al.*, 2007) and insensitive g_{sn} (Barbour & Buckley, 2007) to increasing vapour pressure deficit (VPD) and CO_2 (Zeppel *et al.*, 2012; Resco de Dios *et al.*, 2013b). These behaviours suggest a responsive role to g_{sn}, which only occurs at night, overriding normal daytime response.

Moreover climate change is resulting in global nocturnal (minimum, T_{min}) temperatures rising up 1.4-fold faster than daytime temperatures (Peng *et al.*, 2004; Sillmann *et al.*, 2013; Screen, 2014; Davy *et al.*, 2017) leading to significant yield losses for major crop species such as rice (Welch *et al.*, 2010) and wheat (Lobell & Ortiz-Monasterio, 2007; García *et al.*, 2016). For a recent review, see Moore *et al.* (2021). These increases in T_{min} are having a greater impact on yield than daily maximum temperatures (T_{max}; Cossani & Reynolds, 2013; Martre *et al.*, 2017). However, little consideration has been given to g_{sn} at different stages of development. In wheat, most research has focussed on the impact of rising T_{min} on the reproductive growth stages (e.g. anthesis and grain filling), reporting between 4% and 10% yield losses for every 1°C increase in T_{min} for winter (Hein *et al.*, 2019) and spring wheat (Lobell & Ortiz-Monasterio, 2007; García *et al.*, 2016). Any increases in diurnal ambient temperature are usually accompanied by increases in water use and loss by crops. At night, plants experience often highly contrasting environmental conditions to those experienced in the day; including significant drops in temperature, high humidity and dew-fall and lowered wind speed (Fig. 1; Jones, 2013).

Accounting for up to 55% of daytime water loss (Caird *et al.*, 2007; Schoppach *et al.*, 2014), g_{sn} occurs in crop and noncrop species alike (Resco de Dios *et al.*, 2019). At a larger scale, land-surface models indicate that an increase in g_{sn} from 0% to 5%

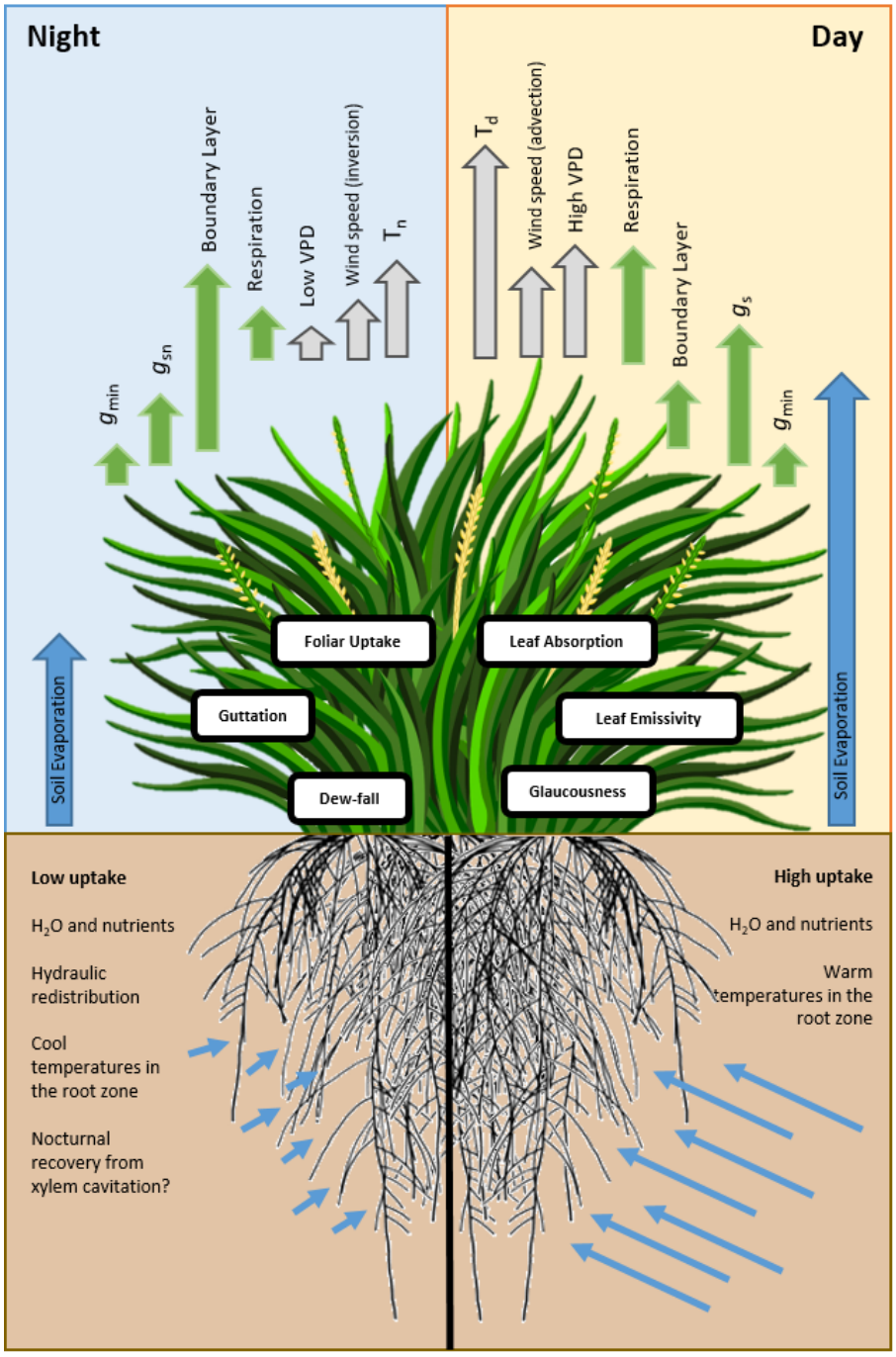

Fig. 1 A schematic summarising the main factors influencing diurnal water movement. At night, low temperatures, low vapour pressure deficit (VPD) and wind speed culminate in low boundary layer conductance. Accordingly, high boundary layer resistance limits the rate of nocturnal transpiration (T_n), stomatal conductance (g_{sn}) and minimum leaf conductance (g_{min}). Under the cooler nocturnal temperatures, the canopy also experiences lower rates of respiration and less water loss from the soil. The soil is cooler and hydraulic redistribution may occur in the root zone. As dawn approaches, dew-fall and guttation can occur as water vapour in the air condenses on the cooler leaf surface and hydathodes expel concentrated solutions to a near water vapour saturated boundary layer. Foliar uptake of H_2O occurs in some species, providing an alternative water supply to the aerial parts of the plant. As the sun rises, temperatures and wind speeds increase, leading to high VPD and low boundary layer resistance. These conditions promote high rates of soil evaporation, root water uptake, transpiration and stomatal conductance. Under these conditions, characteristics such as high leaf emissivity and glaucousness serve to deflect high intensity solar radiation, cooling the leaf to maintain low levels of photorespiration, protect from photoinhibition and mediate evaporative cooling under increased temperature loads. Schematic modified from images created by Carvalho (2019) and Lobell (2017). Arrows indicate plant (green), soil (blue) and environment (grey)-centric processes.

could account for a reduction in available soil moisture of up to 50% in semiarid areas, emphasising the vital but often overlooked role of g_{sn} in large-scale water systems as many models assume g_{sn} to equal 0 (Lombardozzi *et al.*, 2017). Although high g_{sn} appears indicative of low water-use efficiency (Claverie *et al.*, 2018; Schoppach *et al.*, 2020), as yet, a single species-wide role of g_{sn} has yet to be established (Caird *et al.*, 2007; Fricke, 2019; Resco de Dios *et al.*, 2019).

Roles for g_{sn} have been proposed: positive correlations have been observed between g_{sn} and the breakdown of starch (Easlon & Richards, 2009; dos Anjos *et al.*, 2018) and a role in the maintenance of growth (Fricke, 2019); promoting continuous water flow from the roots, aiding nutrient uptake and distribution while maintaining the turgor required for expansion (Donovan *et al.*, 2001; Snyder *et al.*, 2003; Marks & Lechowicz, 2007). Conversely, high g_{sn} has also been shown to reduce hydraulic redistribution, limiting transpiration the following day. This could culminate in reduced plant productivity if daily water-use efficiency (W_i) is low (Howard *et al.*, 2009). Noted by Resco de Dios *et al.* (2016), g_{sn} is often higher pre-dawn than post-dusk,

leading to the conclusion that this behaviour also serves to maximise carbon acquisition at dawn when VPDs are low (Resco de Dios *et al.*, 2016; Schoppach *et al.*, 2020). This antecedent response highlights a potential role for g_{sn} to coordinate daytime exchange of CO_2 and H_2O in response to either a circadian cue (e.g. dawn or dusk) or a consistent but short-term event, for example heatwaves, increased soil water availability or decreased availability of starch under low CO_2.

As g_s regulates the exchange of CO_2/H_2O during the day, g_{sn} could be a potential mechanism for facilitating the uptake of O_2 and release of respiratory CO_2 at night. With up to 70% of daily net photosynthetic carbon fixation estimated to be re-released via respiration in the following evening (Atkin *et al.*, 2005, 2007; Liang *et al.*, 2013), g_{sn} could play a part in facilitating nocturnal cellular expansion and repair (Daley & Phillips, 2006; Even *et al.*, 2018; Fricke, 2019). Recently an optimisation model was proposed based upon trade-offs between leaf temperature, evaporative cooling and respiration (Wang *et al.*, 2021).

While the number of publications into crop g_{sn} is growing (Resco de Dios *et al.*, 2019), most studies have focussed on the response of g_{sn} in specific developmental periods, for wheat the reproductive growth stages (booting to anthesis). Clearly different growth stages in wheat represent substantial changes in above and below ground architecture, metabolic capacity and hydraulic conductance. Understanding the magnitude of g_{sn} and whether it changes with phenology is vital in identifying a role for g_{sn} but also in generating targets for improving heat and drought tolerance. We hypothesise that nocturnal water loss in the earlier growth stages could have important implications for establishment and relative growth rate when sensitivity to temperature changes is greater, due to the smaller size of the plants (Slafer & Rawson, 1995). We also hypothesise that g_{sn} is higher in genotypes with intrinsically higher g_s and lower W_i a relationship that has not been fully established (Rawson & Clarke, 1988; Schoppach *et al.*, 2014; Resco de Dios *et al.*, 2019). A final omission in the assessment of g_{sn} is the use of realistic and appropriate conditions for precise experimentation over diurnal periods. To overcome this we utilised state-of-art controlled environment technology to simulate realistic diurnal fluctuations in light and temperature. The objective of this study was first to investigate genotype-specific differences in g_{sn}, assessing the contribution of g_{sn} for a modern *T. aestivum* and wild relative, *T. urartu*. Eight wheat cultivars were then investigated for genotypic variation in g_{sn} under simulated conditions of north-western Mexico, and whether these differences were growth-stage specific. g_{min} was assessed for each cultivar at flag leaf to determine the contribution of g_{min} to g_{sn} for each genotype. Finally, variation in stomatal density, size and ratio were determined, along with harvest characteristics.

Materials and Methods

Diurnal glasshouse measurements

Plants were grown and analysed at Sutton Bonington Campus, University of Nottingham during the period 7–15 November 2019. Five wild relative plants, *Triticum urartu* (accession no. 1010001) and five modern spring wheat cultivar, *T. aestivum* 'Paragon', were potted into soil (John Innes No. 2; J. Arthur Bowers, UK) and drip irrigated twice per day for 1 min with Hoagland's solution. Glasshouse conditions were maintained at 25/18°C ± 2°C (day/night) under regular mildew, aphid and thrip control measures. Photosynthetic photon flux density (PPFD) was maintained to achieve 16 h of light using supplemental lighting (Son-T; Philips, Surrey, UK), applying up to 250 μmol m^{-2} s^{-1} PPFD at plant height when ambient PPFD fell below 500 μmol m^{-2} s^{-1}. During the measurement period, maximum PPFD at chamber height ranged between 143.7 and 484.0 μmol m^{-2} s^{-1}.

Using the flag leaf – decimal growth stage 39–40, as defined by the UK HGCA (AHDB) growth-stage guide, which is based on the Zadoks 100 point growth scale (Zadoks *et al.*, 1974; AHDB, 2018) – the ambient response of A/R_d and g_s/g_{sn} was monitored using an infrared gas analyser (IRGA) (LI-6800; Li-Cor, Lincoln, NE, USA) fitted with a clear-topped chamber. Leaf areas for the modern genotype were between 4.8–6 cm^2 and 1.5–2.4 cm^2 for *T. urartu*. To enable true assessment of g_s and g_{sn} to ambient conditions, a carboy bottle buffered the ambient air from the glasshouse to the IRGA. As such, CO_2 concentration was not controlled within the chamber. Measurements were taken every 5 min with a match every 30 min for 24 h. Due to the small signal-to-noise ratio of the *T. urartu* samples, measurements of R_d were discounted from the analysis and discussion.

One wild relative plant and one modern genotype were measured per 24 h period using two IRGAs. Key diurnal periods were compared between replicates; dusk (1 h before sunset: 21:00–22:00), dawn (1 h after sunrise: 06:00–07:00) and post dawn (4 h after sunrise: 10:00–11:00).

Growth room conditions and plant material

Six modern spring wheat cultivars were chosen: 'Paragon', 'Cadenza', 'Pavon76', 'Vorobey', 'Sokoll' and 'Borlaug100'. The latter three are common high yielding check cultivars grown in the Yaqui Valley (Obregon, Sonora, NW Mexico) as part of CIMMYT field trials. Two Watkins landraces were also selected with reported high (accession no. 468-W468) and low (accession no. 483-W483) intrinsic water-use efficiency. Seeds were stratified for 3 d on damp filter paper at 5°C, sown into compost (Levingtons, M3, Everris, Ipswich, UK). After 2 wk, seedlings were potted into loam soil representative of the Centro Experimental Norman E. Borlaug (CENEB) research station (Yaqui Valley, Sonora, Mexico; 27.370°N, 109.930°W). Plants were randomised and drip irrigated for 3 min 3× day^{-1}, increasing to 4 min at heading and 5 min at anthesis. When 80% of plants were at anthesis, a high nitrogen fertiliser was applied for the remainder of the growing period (5% OMEX Standard; OMEX Agriculture Ltd, Kings Lynn, UK).

To simulate Mexican monthly temperature fluctuations the average T_{min} and T_{max} ambient temperatures were calculated for the months December (sowing) to April (harvest) for 2014–2018 as obtained from a field weather station (2016–2018, CIMMYT,

Obregon, Sonora, Mexico) and a weather location located at Obregon airport (2014–2016, 18 km from the field station). These values were then applied to the model of Campbell & Norman (2012) to simulate the daily changes in temperature (Campbell & Norman, 2012; Fig. 2a) while humidity was maintained at 67.2% (±4.5%) with a mean VPD of 0.73 ± 0.35 kPa. PPFD was determined following a three-parameter Gaussian sigmoidal function (Fig. 2b), applying a maximum of 1000 μmol m^{-2} s^{-1} at solar noon (12:30 h) and providing a photoperiod of 16 h : 8 h, light : dark. This response was staggered to allow pre-dawn gas-exchange measurements to occur within normal working hours of 08:00 to 18:00. Carbon dioxide concentrations were also closely monitored (Fig. 2c). While mean ambient CO_2 slightly increased between December and March, the maximum mean increase was 4.8 ppm (1.1%) and reflected an increase in measurements. CO_2 then declined in February to April to concentrations similar to those observed at the start of the experiment. Gas-exchange measurements inside the growth room were limited to maximum 2 h with no return within 1 h to prevent prolonged leaf exposure to high [CO_2].

Gas-exchange measurements

Cultivars were measured within specific growth-stage periods as characterised using the decimal growth-stage system; pre-flag leaf ('Pre-GS39' – GS29-38), fully expanded flag leaf ('GS39' – GS39-42), heading (GS51-59) and anthesis (GS61-69). Only the main and second tiller of each plant were measured. Using an infrared gas-exchange system and a 2 cm^2 leaf chamber with an integral blue–red LED light source (LI-6400-40; Li-Cor), leaves were measured under ambient conditions 1 h before dawn and 4 h after dawn. For the pre-dawn measurements, leaves were selected with the aid of a dimmed head torch (< 2 μmol m^{-2} s^{-1} PPFD at a distance of 50 cm) placed in the dark chamber under a flow of 300 ml min^{-1} at 12.4 ± 0.44°C leaf temperature, 55.0 ± 4.41% RH, 400 ppm extracellular CO_2 (C_a). For the post-dawn measurements, leaves were illuminated with 1000 μmol m^{-2} s^{-1} PPFD and measured under a flow of 500 ml min^{-1} at 16.3 ± 0.74°C leaf temperature and 62.5 ± 2.56% RH, 400 ppm C_a. For all measurements, leaves were held in the chamber for no more than 3 min. To distinguish between adaxial and abaxial surface, porometer (SC-1, Decagon Devices, Pullman, WA, USA) measurements of g_{sn} and g_s at booting (GS40-49) and anthesis were made for the adaxial and abaxial leaf surfaces. However, to ascertain concurrent rates of g_{sn}/R_d or g_s/A, IRGA measurements were prioritised.

Cuticular or minimum conductance – g_{min}

Following the method of Sack *et al.* (2003), all measurements were made on fully expanded flag leaves, sampled from the second tiller 2 h post dawn. The excised ends were dipped in wax, photographed for area and weighed to 4 dp. These leaf sections were placed on coarse wire mesh shelving in a dark growth cabinet at 43.1 ± 1.4% RH and 25.9 ± 1.0°C for 1 h to close stomata. The mesh shelving allowed airflow to both sides of the leaf without damaging the leaf surface. Leaf sections were then weighed at intervals of 20 min over a period of 5 h and placed back on the mesh, alternating the sides that faced upwards for maximum contact with the circulating air. Cuticular transpiration was measured as the slope of water loss vs time; the slope of the decline from 2 to 4 h was used to estimate cuticular transpiration. The value of g_{min} was calculated as the rate of cuticular transpiration divided by the mole fraction gradient in water vapour from the leaf to air, assuming the leaf internal air to be fully saturated (Pearcy *et al.*, 2000; Sack *et al.*, 2003). Ambient

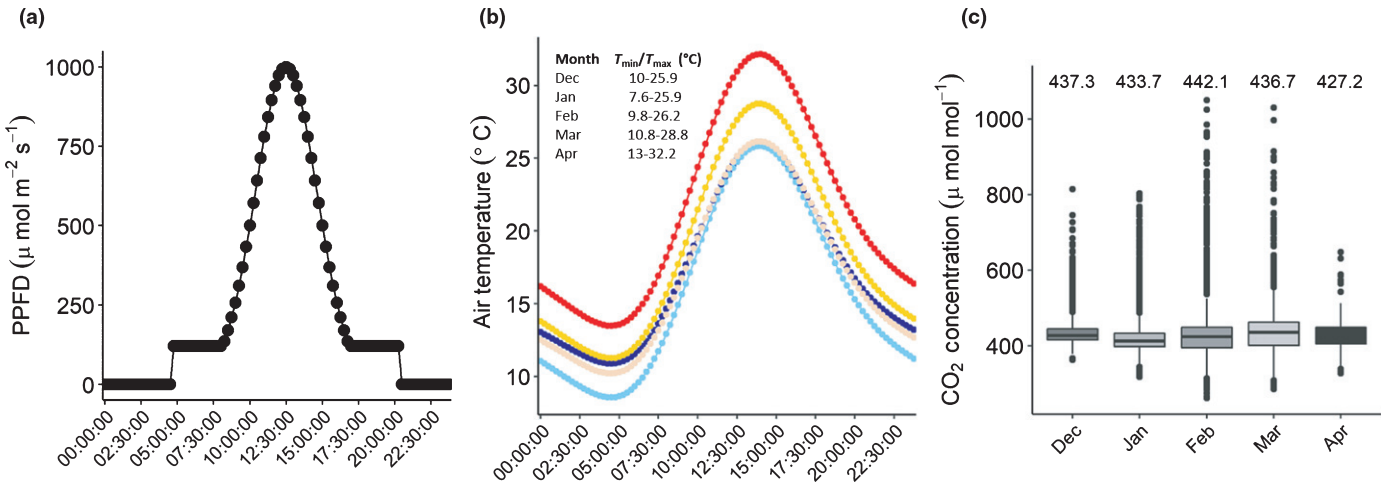

Fig. 2 Simulated environmental conditions to mimic monthly fluctuations for a field in Obregon, Sonora, Mexico. (a) The response of photosynthetic photon flux density (PPFD) was maintained throughout at a maximum of 1000 μmol m^{-2} s^{-1}. Daily T_{min} and T_{max} were changed per month (b) for December (dark blue), January (light blue), February (pink), March (yellow) and April (red), according to average values established between 2014 and 2018 from weather stations on or close to a CIMMYT field site (Obregon, Sonora, Mexico). [CO_2] in the growth room was also monitored every 15 min (c) throughout the growing period. Boxplots show the median (horizontal line), the quartiles (boxes). The whiskers represent 1.5-times the interquartile range above and below the 75th and 25th percentile respectively, with extreme values indicated as dots, measured during measurement periods. The mean [CO_2] for the month is indicated above each boxplot.

temperature and RH were measured at leaf height every minute (TinyTag, Gemini Data Loggers, Chichester, UK).

Stomatal density, size and ratio

Stomatal impressions of the flag leaf (GS39-40) adaxial and abaxial leaf surfaces were taken of the same area using clear nail varnish. The abaxial surface was identified as the surface with the most prominent midrib for each leaf. The impression was removed using clear tape onto a microscope slide. Stomata were counted from 10 fields of view at ×200 magnification per sample (total area: 1250 μm^2). Stomatal density and measurements of pore length, guard cell width enabled the estimation of anatomical maximum stomatal conductance to water (g_{smax}; Parlange & Waggoner, 1970; Franks & Beerling, 2009). Measurements were obtained using ImageJ (Rasband, 1997–2018) software at a scale of 5.36 pixel μm^{-1}. Stomatal ratio was calculated as the number of stomata found on the adaxial to abaxial surfaces of the leaf.

Biomass and yield

Seeds and dry biomass were harvested *c.* 2.5–3 wk post anthesis. Ears were removed and counted for each plant, Three ears were weighed per plant and then all ears were threshed. The total seed weight and number was recorded. Harvest index was calculated as the total grain yield per plant to total aboveground dry biomass (Thomas & Prasad, 2003). Plant height and tiller number was recorded into leaf or stem material that was placed in a drying oven at 70°C for 72 h and weighed.

Statistical analyses

Statistical analyses were conducted in R (http://www.r-project.org/). A Shapiro–Wilk test was used to test for normality and a Levene's test of homogeneity was used to determine if samples had equal variance. Single factor differences were analysed using a one-way ANOVA with a Tukey–Kramer honest significant difference (HSD) test where more than one group existed or using Student's *t*-test in which only two groups were compared. For linear correlations, Pearson's correlation coefficient was calculated. All replicate numbers reported are biological replicates. A correlation matrix was calculated for all measured parameters using either an average over all the measurements or separated by growth stage. For visualisation, only significant ($P < 0.05$) pairwise Pearson correlations with significance are shown. The matrices were created using the R package corrplot (Wei & Simko, 2016).

Results

T. urartu demonstrates significantly higher g_{sn} compared with *T. aestivum*

To ascertain whether variation in g_s and g_{sn} exists between two closely related species, diurnal gas-exchange measurements were made on the flag leaves of wild relative, *T. urartu*, and modern cultivar *T. aestivum* 'Paragon' (Fig. 3a). During the day, *T. urartu* demonstrated significantly ($P < 0.05$) higher mean g_s (Fig. 3b; 0.384 ± 0.097 mol m^{-2} s^{-1}) and rates of CO_2 assimilation (Supporting Information Fig. S1; 3.79 ± 1.14 µmol m^{-2} s^{-1}), more than 4-fold and 1.5-fold higher than those observed for *T. aestivum* (0.098 ± 0.013 mol m^{-2} s^{-1} and 2.59 ± 0.49 µmol m^{-2} s^{-1}, respectively). At night, mean values of g_{sn} were also 3.3-fold higher in *T. urartu* (Fig. 3c, 0.021 ± 0.014 mol m^{-2} s^{-1}) compared with *T. aestivum* (0.006 ± 0.004 mol m^{-2} s^{-1}).

The diurnal data were split into key periods to determine the impact of the magnitude of g_s and g_{sn} on the rates of photosynthesis and respiration respectively. During the day, mean responses of A and g_s were determined for 1 h after sunrise ('dawn'), 4 h after dawn and 1 h before sunset ('dusk'). *T. urartu* was able to maintain significantly higher rates of g_s ($P < 0.0001$) for all three periods (Fig. 3b), enabling significantly ($P < 0.0001$) greater rates of carbon acquisition in these periods (Fig. S1). However, consistently high rates of g_s resulted in *T. urartu* demonstrating values of W_i 2.8-fold lower than that measured for *T. aestivum* during the day (Fig. 2d, 0.011 ± 0.004 mol CO_2/mmol H_2O m^{-2} s^{-1} and 0.029 ± 0.007 mol CO_2/mmol H_2O m^{-2} s^{-1} respectively).

At night, the diurnal data were split into two further periods of interest: 1 h after dusk and 1 h before dawn. Again, *T. urartu* was able to maintain significantly ($P < 0.0001$) higher g_{sn} during both periods (0.035 ± 0.04 and 0.017 ± 0.03 mol m^{-2} s^{-1} respectively); these values were 4.4-fold and 3.1-fold greater than the values observed for Paragon for the same periods (Fig. 3c). At 1 h before dawn, *T. urartu* g_{sn} values were 33.3% lower than the values observed after dusk, while for Paragon this decrease was 55.3%.

Nocturnal conductance in elite lines is genotype and growth-stage specific

Six modern spring wheat varieties and two Watkin's Landraces were measured before and after dawn during six growth stages. Porometer measurements of g_{sn} at booting and anthesis determined that adaxial g_{sn} was significantly higher than abaxial g_{sn} in six of the eight genotypes measured for pre-dawn g_{sn} (Fig. S2a) and four of the eight for post-dawn g_s (Fig. S2b). To our knowledge, this is the first report of this behaviour in wheat. However, to ascertain concurrent rates of g_{sn}/R_d or g_s/A, IRGA measurements were prioritised.

Combining gas-exchange data across all growth stages, significant differences were noted between the genotypes for both g_{sn}, g_s (Fig. S3a,b, $P < 0.007$), A and R_d (Fig. S3c,d; $P < 0.02$). In brief, Borlaug100 demonstrated significantly higher g_{sn} across all growth stages ($P < 0.01$; 0.063 ± 0.048 mol m^{-2} s^{-1}) when compared with all other cultivars, with W468 demonstrating the lowest mean g_{sn} (0.023 ± 0.019 mol m^{-2} s^{-1}). During the day, Pavon76 had the highest g_s (0.502 ± 0.176 mol m^{-2} s^{-1}), which was only significantly higher than Vorobey and Paragon ($P < 0.03$). No significant differences were found between the individual genotypes for R_d, while Pavon76 achieved the highest

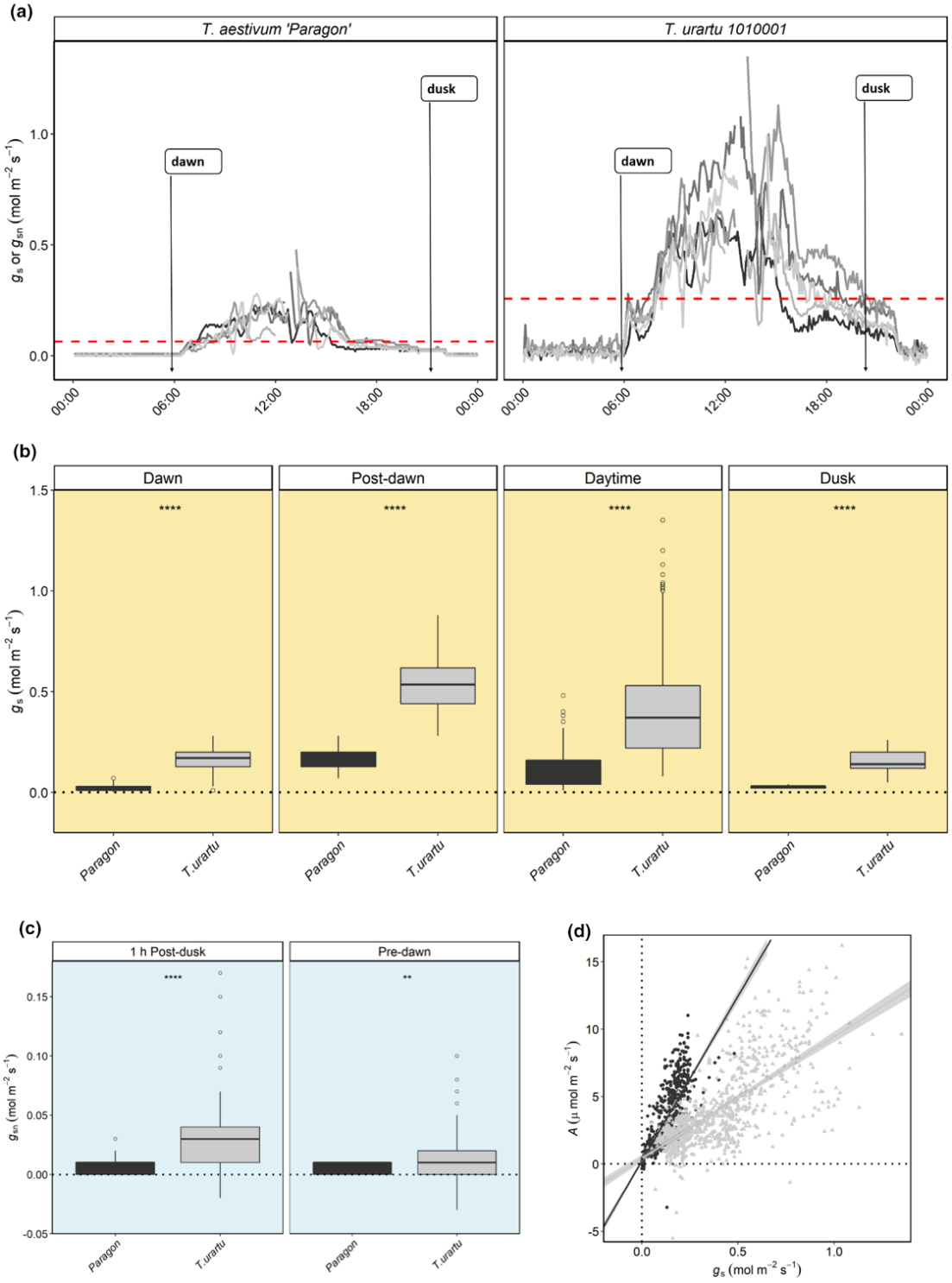

Fig. 3 The diurnal responses of (a) stomatal conductance (g_s) in five biological replicates of modern genotype *Triticum aestivum* '*Paragon*' and wild relative *T. urartu* 1010001 over 5 days – the red dotted line indicates the mean stomatal conductance for all measurements taken for each genotype. The response of the two genotypes was analysed at set periods during the day (b; see the Materials and Methods subsection Diurnal glasshouse measurements). *T. urartu* demonstrated significantly higher values of g_s 1 h post sunrise ('Dawn'), during the day ('Daytime') and 1 h before sunset ('Dusk'). In addition, *T. urartu* also demonstrated significantly higher nocturnal conductance (c – g_{sn}) compared with the modern genotype during the period 1 h post-dusk and 1 h pre-dawn ('Pre-dawn'). Measurements are individual data points ($n = 5$). Boxplots show the median (horizontal line), the quartiles (boxes). The whiskers represent 1.5-times the interquartile range above and below the 75th and 25th percentile respectively. A *t*-test was performed and asterisks indicate the following levels of significance: ****, $P < 0.0001$; ***, $P < 0.001$; **, $P < 0.01$; *, $P < 0.05$. When comparing (d) daytime CO_2 assimilation (A) and g_s between genotypes, consistently higher g_s led to low intrinsic water-use efficiency in the *T. urartu* (grey triangles) compared with Paragon (black circles). The dotted line on (b–d) indicates zero g_s or g_{sn}.

values of A ($P < 0.05$) when compared with Paragon and the two Watkin's lines.

When comparing the ratio of R_d/A, a significant negative correlation was observed ($R^2 = -0.48$; $P = 0.002$). Although this relationship was not found to be genotype specific ($P = 0.439$), there was a general trend observed between growth stage and R_d/A ratio, with younger growth stages (<GS39, GS39) having higher values compared with older material (Heading and Anthesis; Fig. S4) however, no significant differences were observed between the growth stages ($P = 0.47$).

Separating the data by growth-stage highlights additional trends (Fig. 4). There was a general trend for decreasing conductance with age, both at night (Fig. 4a) and during the day (Fig. 4b), however this decrease was genotype specific. Vorobey demonstrated the greatest decrease in mean g_{sn} and g_s between <GS39 and anthesis (80.24% and 67.04% respectively), while the smallest decreases were observed for Pavon76 (31.32%) and Borlaug100 (21.13%).

Five of the eight cultivars indicated significant differences ($P < 0.05$) in g_{sn} between growth stages (Figs 4, S5). Most significant comparisons were between <GS39 and heading. No significant differences were noted between <GS39 and GS39. For the post-dawn measurements, seven of the eight cultivars indicated significant ($P < 0.04$) differences in g_s between growth stages. Growth stages <GS39 and GS39 also achieved values of g_s, which were significantly ($P < 0.04$) higher than booting, emergence and anthesis in the majority of cases. Borlaug100 was the only cultivar to show no significant difference in g_s throughout <GS39 to anthesis ($P = 0.23$). In summary, the magnitude of g_{sn} was genotype specific, accounting for between 5.7% (±2.1%) to 18.9% (±3.6%) of the g_s values 4 h after dawn.

In general, genotypes with the greatest mean g_{sn}, saw the greatest percentage decreases in the proportion of g_{sn} to g_s as the plants aged, for example g_{sn} in Borlaug100 fell from 16.9% of post-dawn g_s at <GS39 to 9.6% g_s at anthesis. Conversely, those plants in which mean lifetime g_{sn} was low (<0.027 mol m^{-2} s^{-1}), g_{sn} made up a greater proportion of water loss as these plants reached anthesis; Paragon achieved one of the lowest mean g_{sn} during its lifetime (0.03 mol m^{-2} s^{-1}) – however, it demonstrated the second greatest decline in g_s from <GS39 to anthesis (65%). Subsequently, g_{sn} climbed from 9% of daily g_s to 14.7%.

Significant positive relationships were noted between A and g_s (Fig. 5a) and g_s and g_{sn} (Fig. 5b). A significant negative correlation was noted between R_d and g_{sn} (Fig. 5c) and between R_d and A (Fig. S4; $R^2_{adj} = -0.48$, $P = 0.002$) between the genotypes grown in the growth room. No significant relationship was determined between mean lifetime A and g_{sn} (Fig. S6a; $R^2_{adj} = 0.44$, $P = 0.27$), however a significant positive correlation was determined between g_{sn} at GS39 (R^2_{adj}: 0.71, $P = 0.05$) and booting (R^2_{adj}: 0.87, $P = 0.014$) and A achieved at anthesis (Fig. S6b).

This decrease in g_s and A over time was accompanied by significant increases in W_i over time (Fig. S7). With the exception of Borlaug100 and W483, all genotypes demonstrated between a 51.0% (Pavon76) and 89.9% (Vorobey) increase in W_i when comparing <GS39 and anthesis. While W468 and W483 were selected were due to high and low water-use efficiency in the field, there was no significant difference in W_i between these genotypes ($P = 0.21$), nor was any single growth-stage W_i was

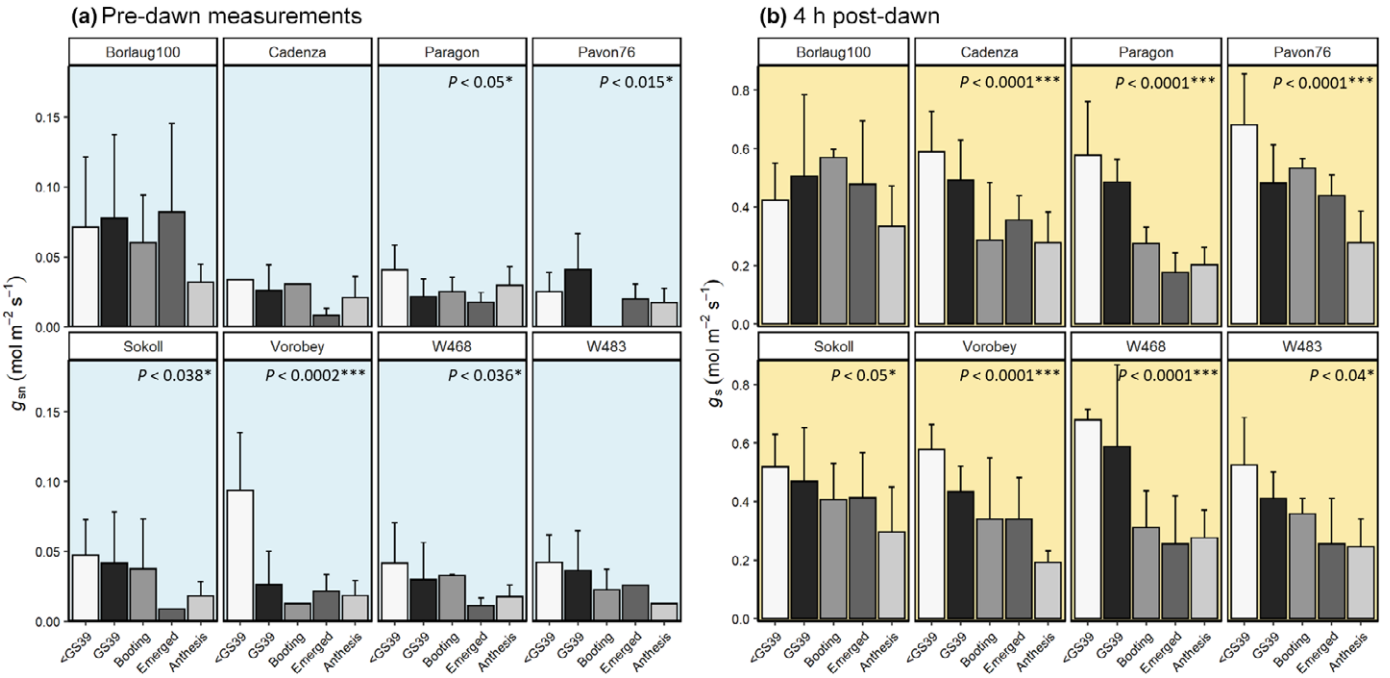

Fig. 4 The responses of (a) pre-dawn (g_{sn}) and (b) 4 h post-dawn (g_s) stomatal conductance in six modern spring wheat genotypes and two Watkins landraces (W468 and W483) from tillering (<GS39) to anthesis. The stomatal conductance data for each genotype is separated into five broad growth stages (see Gas-exchange measurements section for more details). Significant differences ($P < 0.05$) are indicated in the top right hand corner of each plot. Asterisks indicate the following levels of significance: ***, $P < 0.001$; **, $P < 0.01$; *, $P < 0.05$. Data are the means with standard deviation ($n = 4$–6).

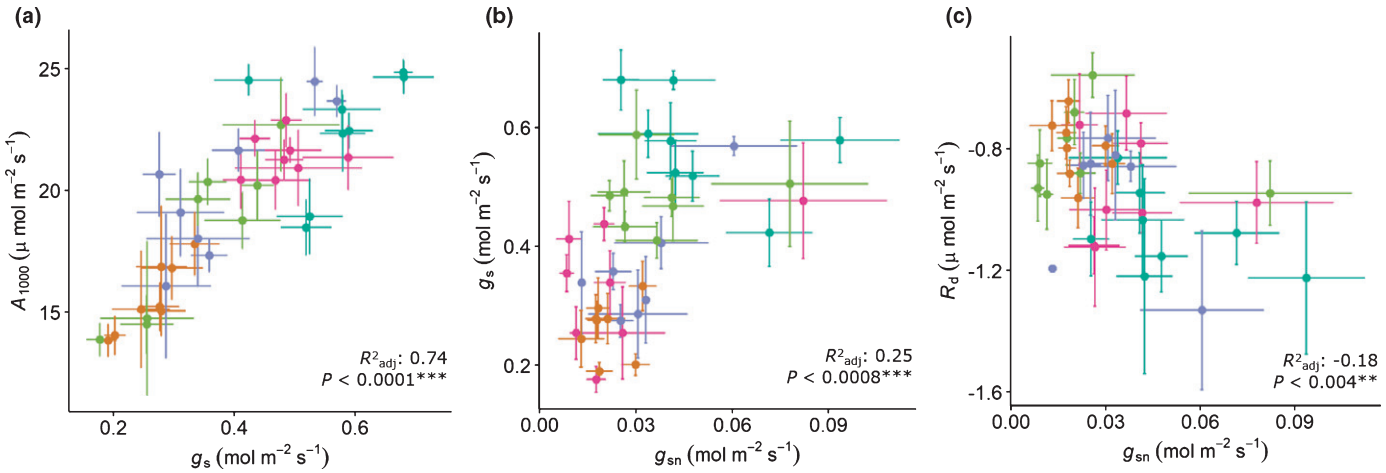

Fig. 5 The growth-stage specific relationship between (a) CO_2 assimilation (A) and stomatal conductance (g_s) under 1000 μmol m^{-2} s^{-1} PPFD, (b) the relationship between pre-dawn g_s (g_{sn}) and g_s and finally, (c) the rate of respiration (R_d) and g_{sn}. Data are the means (n = 4–6) with standard deviation of six modern spring wheat genotypes and two Watkins landraces (W468 and W483) and indicate the following growth stages; pre-flag leaf (dark green), flag leaf (light green), booting (purple), heading (dark pink) and anthesis (orange). The coefficient of determination (R^2 value) was determined for each relationship and is shown in the bottom right corner of the plot along with the P-value. Asterisks indicate the following levels of significance; ***, P < 0.001; **, P < 0.01; *, P < 0.05.

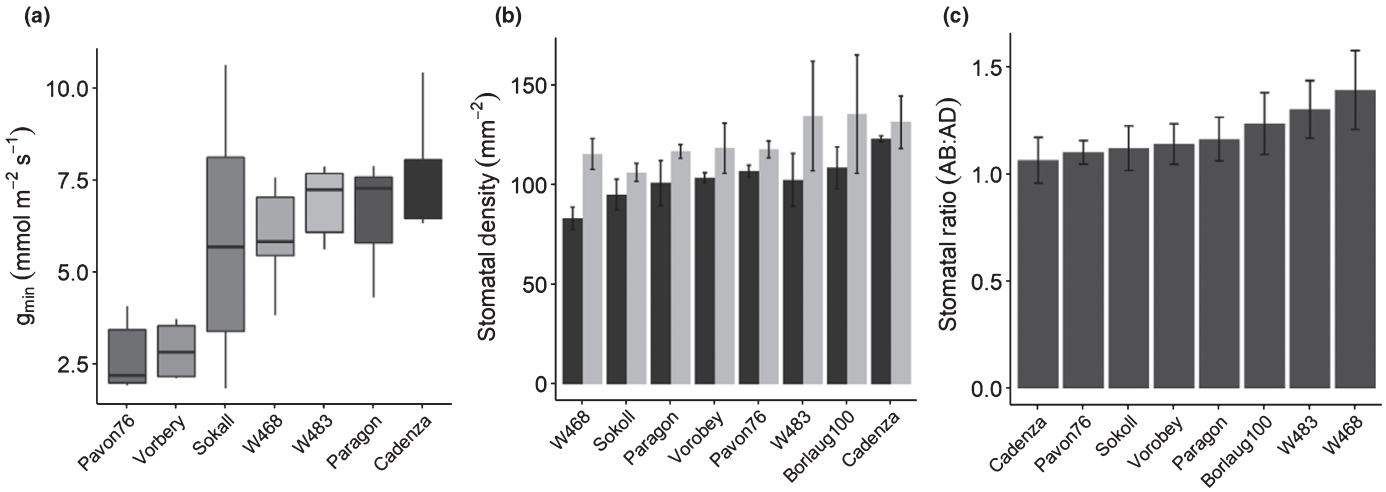

Fig. 6 (a) The minimum conductance (g_{min}), (b) stomatal density on the adaxial (light grey) and abaxial (dark grey) flag leaf surfaces of six modern spring wheat genotypes and two Watkins landraces (W468 and W483). The stomatal ratio, the number of stomata on the bottom of the leaf (AB, abaxial) compared with the top (AD, adaxial) of the eight genotypes was also estimated (c). For (a) boxplots show the median (horizontal line), the quartiles (boxes), while the whiskers represent 1.5-times the interquartile range above and below the 75th and 25th percentile respectively. For (b) and (c), data are the means (n = 4–6) with standard deviation.

significantly different when comparing these two Watkins lines. However, there was a significant effect of growth stage within each of the other six genotypes measured (P = 0.003). Combined, W_i was also not significantly different between the Watkins genotypes and the modern genotypes (P = 0.782).

Measurements of cuticular conductance (g_{min}) were performed at flag leaf (GS39-42). Measurements of g_{sn} at flag leaf were on average 3.3-fold (Paragon) to 15-fold (Pavon76) higher than measurements of g_{min} (Fig. 6a), suggesting that while g_{min} does contribute to nocturnal water loss, stomata at this growth stage are actively open at night. g_{min} was also significantly different between genotypes (P = 0.003) with cadenza reporting the greatest values (0.0077 ± 0.0017 mol m^{-2} s^{-1}) and Pavon76 the lowest (0.0027 ± 0.0009 mol m^{-2} s^{-1}).

Flag leaf stomatal density and ratio were also collected from all eight genotypes (Fig. 6b,c). Genotype-specific significant (P < 0.05) differences in stomatal density were only observed when comparing the abaxial (lower) leaf surfaces. In general, abaxial pores and guard cells were shorter (Fig. S8a) and thinner (Fig. S8b) with smaller estimated pore area (Fig. S8c). The smaller size and density of the abaxial guard cells culminated in smaller abaxial g_{smax} for the majority of genotypes (Fig. S8d). Significant differences were found between the genotypes for all four parameters (P < 0.001). While A was found to positively

correlate ($P = 0.01$, $R^2_{adj} = 0.82$ – Fig. S6a) with abaxial g_{smax} and height negatively correlated with abaxial g_{smax} ($P = 0.02$, $R^2_{adj} = -0.78$; Fig. S6a), there was no significant correlation ascertained between the stomatal measurements and g_{sn} when culminating the data across the lifetime of the plants. In terms of growth-stage-specific comparisons, only adaxial g_{smax} and guard cell width was found to positively correlate with g_{sn} at heading ($P = 0.05$, $R^2_{adj} = 0.71$; Fig. S6b) and flag leaf ($P = 0.05$, $R^2_{adj} = 0.71$; Fig. S6b) respectively.

For all genotypes, there were more stomata on the adaxial surface than on the abaxial surface resulting in stomatal ratios > 1, despite the greater g_{sn} observed from the adaxial surface in most lines. These ratios were only significant for Pavon76, W468 and Sokoll.

A significant positive correlation was observed between stomatal density and seed number (Fig. S9; $R^2_{adj} = 0.71$, $P = 0.05$). Conversely, a negative significant correlation was observed between stomatal ratio and seed weight (Fig. S9; $R^2_{adj} = -0.74$, $P = 0.035$); plants with higher stomatal densities on the abaxial surface achieved greater numbers of heavier seed.

Genotype-specific harvest traits

On average, the Watkins genotypes had the fastest rates of development (see Fig. S9), were generally taller than the modern cultivars – 98.3 ± 1.5 cm compared with 81.9 ± 9.7 cm (Fig. S10a), exhibiting the highest number of tillers: 36.5 ± 7.5 cm compared with 20.8 ± 5.1 (Fig. S10b). W483 (41.9 ± 5.2 g) and Paragon (37.2 ± 2.2 g) produced the greatest total dry biomass while Borlaug100 produced the lowest (19.1 ± 1.4 g; Fig. S10c). Stem and leaf dry weight (DW) were consistent amongst all genotypes (34.6 ± 3.6% and 65.4 ± 3.6% of total DW respectively; Fig. S10d). Total DW was negatively correlated with harvest index ($R^2 = -0.89$, $P = 0.003$) and g_s at heading ($R^2 = -0.84$, $P = 0.009$).

While the modern genotypes produced higher numbers of heavier seeds per plant, the Watkins genotypes produced greater numbers of smaller ears with smaller, less numerous seed content (Fig. S10e,f). The modern cultivars produced between *c.* 5 and 25 ears per plant, while the Watkins lines produced *c.* 25–45 (Fig. S10e). Seed weight was negatively correlated with stomatal ratio only ($R^2 = -0.74$, $P = 0.035$).

Harvest index (HI) was significantly different ($P < 0.0001$) between the genotypes; Borlaug100 had the highest HI, significantly (2.12 ± 0.07, $P < 0.05$) higher than the Watkins lines. Although the lowest HI values were observed in W483 (1.00 ± 0.05), these values were not significantly different to modern genotype, Paragon (1.15 ± 0.59). HI was negatively correlated (Fig. S6b) with height ($R^2 = -0.91$, $P = 0.001$) and total DW ($R^2_{adj} = -0.89$, $P = 0.003$). While the genotype with highest lifetime g_{sn} also demonstrated the highest HI (Borlaug100), this relationship was not significant ($R^2_{adj} = 0.62$, $P = 0.09$).

Discussion

Nocturnal conductance still represents a biological enigma that has wide reaching implications for crop water use, especially under conditions of heat and drought. This study has determined genotypic variability in g_{sn} for wheat lines grown under simulated environmental conditions of a north-western Mexican field (Fig. 2). These conditions – which are representative of 40% of wheat grown globally – are characterised by progressively warmer days and cool nights. Under these conditions, a significant positive correlation was observed between g_s and g_{sn} (Fig. 5b), with both measurements declining as the plants aged (Figs 3, 4). The magnitude of g_{sn} was leaf surface and genotype dependent, declining as the plants aged. Cuticular conductance was also genotype specific (Fig. 6a) and significantly lower than g_{sn}.

The diurnal response of g_{sn}

Evidence suggests that g_{sn} has a circadian rhythm; characterised by a decrease in g_{sn} after dusk and an increase in g_{sn} pre-dawn (Caird *et al.*, 2007; Resco de Dios *et al.*, 2013a). This response has been documented for tree species, dicots (Resco de Dios *et al.*, 2015, 2016) and for crops such as maize (Tamang & Sadok, 2018) and wheat (Schoppach *et al.*, 2014; Claverie *et al.*, 2016). Diurnal measurements provide key information on any antecedent behaviour of g_{sn} and highlight any coordinated relationships with g_s, photosynthetic carbon uptake and respiratory carbon release.

In this study, high g_{sn} in the wild relative (*T. urartu*) was positively correlated with high g_s (Fig. 3), which was also reflected in the genotypes measured in growth room study (Fig. 5b) and has been reported in the literature (Cavender-Bares *et al.*, 2007). The relationship between high g_s and g_{sn} has been linked to increases in specific leaf area (SLA; Tamang & Sadok, 2018) and relative growth rate (Resco de Dios *et al.*, 2019). In general, the wild relatives of modern wheat tend to have higher SLA (McAusland *et al.*, 2020) compared with their modern counterparts; supporting the observation that high g_s and g_{sn} maintain a resource-acquisitive strategy under well watered conditions (Cheng *et al.*, 2016).

Despite significantly different magnitudes g_{sn} for all time periods studied during the diurnal, both the wild relative and modern cultivar demonstrated a decline in g_{sn} during the night from dusk to before dawn (Fig. 3c). This decrease in g_{sn} contrasts with other species within the published literature, which suggests that stomata close in response to the onset of night and open before sunrise to maximally acquire carbon under low VPD conditions (Resco de Dios *et al.*, 2016). The plants used in this study were not exposed to highly variable VPD and perhaps these results support the findings of those reported by Auchincloss *et al.* (2014) and Hassidim *et al.* (2017); with *A* being more limited by biochemical processes than the rate of stomatal opening in the period after dawn. While slow stomatal closure at the onset of night could play a role in maintaining hydraulic processes, a decline in g_{sn} pre-dawn may indicate a water-conservative approach to sunrise or a response to low temperature (Agurla *et al.*, 2018).

There are significant, species-specific differences in the rate of stomatal closure and opening in response to light (McAusland *et al.*, 2016, 2020). In species with dumbbell or graminaceous guard cells, there is a significant positive correlation with the

magnitude of opening or closing and the maximum rate of response. There is also evidence that the higher the initial g_{sn} the more rapid the opening when exposed to an increase in light (Wachendorf & Küppers, 2017). There may be a trade-off between the magnitude of stomatal opening pre-dawn (and subsequent water loss) and the rate of opening in response to dawn. In short, a plant that can rapidly open its stomata in response to dawn does not need to maintain high g_{sn} before dawn. If pre-dawn g_{sn} is negatively correlated with speed of stomatal opening, the magnitude of pre-dawn g_{sn} may reflect prioritisation between water loss and early-morning carbon gain dependent on water availability. The long-term impact of this behaviour has yet to be explored and will depend on many *in vivo* and environmental factors; the speed of photosynthetic induction (and therefore the concentration of intercellular CO_2 - C_i - and RuBisCo activation), the availability of starch (Kwak *et al.*, 2017) and pre-dawn soil water availability due to competition or environmental stresses (Yu *et al.*, 2019). Quantifying variation in response and magnitude of g_{sn} in key nocturnal periods will be critical for screening crops for heat and drought tolerance.

The magnitude of g_{sn} is growth-stage specific

While the magnitude of g_s peaks at leaf maturity and declines towards leaf senescence (Field, 1987), less is known about intrinsic variation in g_s throughout the lifecycle of wheat. From these data, we have determined that g_s declines from vegetative stages towards anthesis for the majority of genotypes (Fig. 4b) – in line with rates of CO_2 assimilation (Fig. S6b) – and that g_{sn} also follows this trend (Fig. 4a). For some genotypes, these declines were not significant, for example Borlaug100, Cadenza and W483. For Borlaug100, the genotype with the highest HI, both g_{sn} and g_s were not significantly different between the growth stages. In general, genotypes with the greatest mean lifetime g_{sn} also saw the greatest percentage decreases in their contribution to daytime g_s.

While high g_s can preclude low water-use efficiency, under well watered conditions high g_s also promotes greater rates of carbon assimilation (Lawson & Blatt, 2014), biomass accumulation and light interception (Blum, 2009; Tricker *et al.*, 2018). With strong positive correlations between g_s and g_{sn}, it is possible that the magnitude of g_{sn} reflects a method for fine tuning gas exchange across each 24 h period to optimise water uptake, growth and water loss during plant lifetime, a hypothesis that is in line with a recent model based on optimisation theory (Wang *et al.*, 2021). While high g_{sn} may improve yield under well watered conditions, it may also reduce heat tolerance under drought conditions by preventing complete plant rehydration before dawn (Kavanagh *et al.*, 2007), especially if insensitive to heating (Rogiers & Clarke, 2013; Claverie *et al.*, 2018). This suggests that although g_{sn} has a role to play in the establishment and growth of the plant, there may be an optimum g_{sn}, one that facilitates the regulation of growth through water uptake/turgor maintenance while demonstrating some sensitivity to temperature and water availability. The plants in this study were maintained under well watered conditions, however declining g_s and g_{sn} after anthesis could reflect a switch in priorities from maintenance of growth to initiation of rapid senescence. More studies are needed to investigate whether these growth-stage specific changes are fine tuned to reflect whole plant priorities under stressed environmental conditions such as heat or drought.

There is a fine balance between photosynthesis, biomass production and respiration (R_d), with leaf-level A strongly coupled to R_d (Wang *et al.*, 2020). In the growth room, nocturnal conductance was found to negatively correlate with respiration (Fig. 5c), with greater values of g_{sn} accompanying smaller rates of CO_2 release in younger leaf material. However, the range of R_d and g_{sn} values are both very small, making it difficult to attribute a simple causal relationship between g_{sn} and CO_2 release. R_d is a key process driving growth processes at night (O'Leary *et al.*, 2017) and is strongly influenced by temperature (Posch *et al.*, 2019) although it has not been determined whether g_{sn} substantially contributes to the nocturnal thermoregulation of leaves at high temperatures or is simply a mechanism to mediate the release of CO_2. Accumulation of CO_2 could inhibit the cytochrome respiration pathway (Resco de Dios *et al.*, 2019) and in the absence of g_{sn}, g_{min} is thought to be insufficient to alleviate increases of CO_2 (Even *et al.*, 2018).

In the work presented here, plants were not exposed to heat stress. R_d is typically more sensitive to changes in temperature than A (Posch *et al.*, 2019), therefore to further investigate the role between g_{sn} and R_d, nocturnal heat and/or drought stress should be applied. Interestingly, while many studies have shown g_{sn} decreasing under drought and heat (Rawson & Clarke, 1988; Cavender-Bares *et al.*, 2007), g_{sn} in wheat has been shown to increase, irrespective of water availability, under small increases in nocturnal VPD (Claverie *et al.*, 2018). This perhaps unexpected response requires more experimentation and highlights that, although variation exists in the plants in this study, even greater variation in g_{sn} may exist in response to different combinations of abiotic stress.

The magnitude of g_{sn} is genotype specific

Significant differences in mean lifetime g_{sn} were observed between the modern genotypes, accounting for between 5.7% and 18.9% of mean daytime g_s, which is consistent with the literature (Duursma *et al.*, 2019) and supports the observation that there is variation to be exploited (Claverie *et al.*, 2018) for drought and heat tolerance in wheat (Sadok & Jagadish, 2020). While the range of g_{sn} was low compared with some studies, it should be noted that these plants still exhibited g_{sn} under controlled, well watered conditions with no changes in water availability or VPD. In addition, under the well mixed conditions of the growth room, it is unlikely that the magnitude of g_{sn} observed in this study reflected differences in boundary layer between the genotypes. In the field, increases in T_{min} and wind speed would exacerbate any water losses at night through increasing the rate of evapotranspiration and reducing the boundary layer. Identifying variation in nocturnal water loss contributes to a growing body of work that nocturnal transpiration is underpinned by a wealth of genetic variation to be exploited for optimising crop water-use efficiency (Duursma *et al.*, 2019; Resco de Dios *et al.*, 2019).

While this variation has mostly been explored in woody species (Daley & Phillips, 2006; Phillips *et al.*, 2010; Coupel-Ledru *et al.*, 2016; Resco de Dios *et al.*, 2016), interest is growing around wheat (Claverie *et al.*, 2018; Schoppach *et al.*, 2020). While the work here mostly focusses on pre-dawn responses, even greater variation in g_{sn} may also be observed at dusk (1 h after sunset) or integrating water losses throughout the night (Fig. 3b).

These genotype-specific differences extended to g_{min} at flag leaf (Fig. 6a), with a >3.8-fold difference between the lowest and highest values, g_{min} did not correlate with g_{sn} but contributed between 6.6% and 30.1% of the value of g_{sn}. This high degree of intraspecific variation suggests that g_{min} should always be assessed with g_{sn} and, as we have shown with g_{sn}, could be growth-stage specific in wheat (Duursma *et al.*, 2019). It was also interesting to note that the magnitude of g_{sn} is perhaps leaf-surface specific (Fig. S2a), with up to 1.2–1.3-fold greater rates of nocturnal water loss from the adaxial surface (0.125 ± 0.04 mol m^{-2} s^{-1}) compared with the abaxial surface (0.051 ± 0.01 mol m^{-2} s^{-1}) despite no consistency with morphology. This trend was also observed for post-dawn measurements, with adaxial g_s consistently higher than abaxial g_s (Fig. S2b). While morphological amphistomaty is thought to provide a gas-exchange advantage, shortening the pathways of CO_2 and H_2O exchange and promoting rapid growth (Drake *et al.*, 2019), it is unclear why the stomatal aperture on the two surfaces of the leaf would respond differently at night. This behaviour could reflect more nocturnal-specific fine tuning of diurnal requirements for gas exchange.

Finally, HI was also genotype specific, demonstrating a significant positive correlation with g_s. With a strong positive correlation between g_{sn} and g_s, these results suggest that although any selection against high g_{sn} may improve drought tolerance or water-use efficiency (Sadok & Jagadish, 2020), there may also be a yield penalty, perhaps through limiting growth rates or dawn carbon acquisition (Resco de Dios *et al.*, 2016, 2019). For this study, variation in g_s under well watered conditions did not show strong correlations with individual harvest characteristics such as biomass, height and grain weight (Fig. S9). However, variation in g_s and g_{sn} may be an indicator of tolerance under water or high temperature stress, with those genotypes able to maintain higher g_s (and g_{sn}) also maintaining cooler canopies and greater yields (Fischer *et al.*, 1998; Lu *et al.*, 1998; Fischer & Edmeades, 2010). This would provide a tractable means of selection for improved genotypes, but using low g_{sn} and/or low g_s under nonstressful conditions.

The relationship between g_{sn}, g_{min} and stomatal characteristics

Cuticular conductance varies between species and is dependent on the growth environment (Sack *et al.*, 2003); decreasing under drought and low humidity (Kerstiens, 1996). g_{min} has also been shown as the primary source of water loss from expanding oak leaves (Kane *et al.*, 2020), therefore it is conceivable that while g_{min} was only up to 15-fold lower than g_{sn} at the flag leaf, it could also vary with age; contributing considerably more water loss in young wheat leaf material.

There are very few data available to link stomatal anatomical characteristics with nocturnal behaviours, with most published literature reporting changes in density and size due to large-scale environmental factors, for example lower densities under warmer temperatures (Rogiers & Clarke, 2013) and higher densities under high VPD (Claverie *et al.*, 2016). While we found significant differences in stomatal density and ratio at flag leaf between the genotypes studied (Fig. 6b,c) these values did not correlate with g_{sn} at flag leaf. Although stomatal size also varied between the genotypes, only adaxial guard cell width positively correlated with flag leaf g_{sn} (Figs S6b, S8).

In amphistomatous species grown under well watered conditions, high adaxial to abaxial (AD : AB) densities have been linked to improving parallel CO_2 diffusion in the leaf, increasing mesophyll conductance and leading to higher rates of carbon acquisition (Drake *et al.*, 2019; Pathare *et al.*, 2020). Although one of the three genotypes to demonstrate significant AD : AB density also had the highest lifetime CO_2 assimilation (Pavon76; Fig. S3), there are too few genotypes in this study to conclusively link this trait with improved carbon acquisition. It is possible that the occurrence of high AD : AB densities may be more common under the optimum conditions presented here. The common observation of lower AD : AB densities generally reflects a need to conserve water by increasing AB densities in the more frequently shaded areas of the plant (Mott *et al.*, 1982), in this way, high AD : AB ratios would not be advantageous under heat or water stress.

Variation in stomatal density is generally accompanied by changes in other anatomical characteristics such as vein density (Claverie *et al.*, 2016) and root epidermal thickness (and aquaporin density) to optimise plant vascularisation in line with water demand. While root physiology are not covered in this work, roots are intrinsically linked to water uptake and the hydraulic status (Wasson *et al.*, 2012) of the aboveground plant; with deeper roots leading to cooler canopies and greater yields (Li *et al.*, 2019). As noted by Claverie *et al.* (2018), wheat grown under high nocturnal VPD demonstrates significantly higher g_{sn} and significantly greater root biomass than plants grown under low VPD, therefore it would not be unsurprising if a link arose between root growth, water availability and g_{sn} for these genotypes. Further analyses of wheat genotypes under water and heat stress conditions need to be conducted to determine whether g_{sn} plays a role in drought or heat tolerance and how g_{sn} interacts with other nocturnal traits to sustain or improve yields.

Conclusions

Here we describe genetic, developmental and morphology-dependent variation in nocturnal stomatal conductance in wheat together for the first time. Our results demonstrate that even under the well watered conditions used, different growth stages in wheat represent substantial variation in leaf-level nocturnal conductance and therefore contribute to aboveground water loss. Not only should this variation be taken into account for modelling crop water-use efficiency and nocturnal water flux, it

should also be considered when selecting for water-use efficiency and for heat- and drought-tolerant genotypes for an increasingly warm climate. To do this, knowledge of trade-offs of high or low g_{sn} with other whole plant processes and with yield under a range of growing environments is required. The use of programmable controlled growth environments to impose realistic thermal regimes – which can uncouple confounding environmental variables – is a powerful tool in dissecting the role of g_{sn} in plants.

Acknowledgements

This project was funded by a UK–Mexico grant from the Newton Fund and the Biotechnology and Biological Sciences Research Council (grant no. BB/S012834/1). KES is funded by the Nottingham BBSRC Doctoral Training Programme. This is a Nottingham Futurefoods Beacon tagged project. We thank Prof. Anthony Hall and Dr Rachel Rusholme Pilcher (Earlham Institute) for suggestions on the Watkins lines, Dr Elizabete Carmo-Silva and Dr Alejandro Perdomo-Lopez (Lancaster University) and the Nottingham BBSRC Wheat Research Centre (University of Nottingham) for the generous provision of seeds and glasshouse plants. We are also grateful to the reviewers for their useful and productive feedback on this manuscript.

Author contributions

LM, GM and EHM conceived the work and planned the experiment. LM, KES and AW collected the data, LM performed the data analysis. LM and EHM wrote the manuscript.

ORCID

Lorna McAusland https://orcid.org/0000-0002-5908-1939
Gemma Molero https://orcid.org/0000-0002-6431-7563
Erik H. Murchie https://orcid.org/0000-0002-7465-845X
Kellie E. Smith https://orcid.org/0000-0002-8569-9142

Data availability

The data supporting the findings of this study are available from the corresponding author, (Lorna McAusland), upon request.

References

Agurla S, Gahir S, Munemasa S, Murata Y, Raghavendra AS. 2018. Survival strategies in extreme cold and desiccation. In: Iwaya-Inoue M, Sakurai M, Uemura M, eds. *Advances in experimental medicine and biology*. Singapore City, Singapore: Springer, 215–232.

AHDB. 2018. *Cereal growth stages and benchmarks*. Warwickshire, UK: Agriculture and Horticulture Development Board. [WWW document] URL https://bit.ly/32Nu7Tx [accessed 23 July 2020].

dos Anjos L, Pandey PK, Moraes TA, Feil R, Lunn JE, Stitt M. 2018. Feedback regulation by trehalose 6-phosphate slows down starch mobilization below the rate that would exhaust starch reserves at dawn in Arabidopsis leaves. *Plant Direct* **2**: e00078.

Atkin OK, Bruhn D, Hurry VM, Tjoelker MG. 2005. Evans review no. 2: The hot and the cold: unravelling the variable response of plant respiration to temperature. *Functional Plant Biology* **32**: 87–105.

Atkin O, Scheurwater I, Pons T. 2007. Respiration as a percentage of daily photosynthesis in whole plants is homeostatic at moderate, but not high, growth temperatures. *New Phytologist* **174**: 367–380.

Auchincloss L, Easlon HM, Levine D, Donovan L, Richards JH. 2014. Pre-dawn stomatal opening does not substantially enhance early-morning photosynthesis in *Helianthus annuus*. *Plant, Cell & Environment* **37**: 1364–1370.

Barbour MM, Buckley TN. 2007. The stomatal response to evaporative demand persists at night in *Ricinus communis* plants with high nocturnal conductance. *Plant, Cell & Environment* **30**: 711–721.

Blum A. 2009. Effective use of water (EUW) and not water-use efficiency (WUE) is the target of crop yield improvement under drought stress. *Field Crops Research* **112**: 119–123.

Caird MA, Richards JH, Donovan LA. 2007. Night-time stomatal conductance and transpiration in C3 and C4 plants. *Plant Physiology* **143**: 4–10.

Campbell GS, Norman J. 2012. *An introduction to environmental biophysics*. New York, NY, USA: Springer Science & Business Media.

Carvalho D. 2019. Cartoon version – *Oropetium thomaeum*. Figshare. doi: 10.6084/m9.figshare.8868473.v1.

Cavender-Bares J, Sack L, Savage J. 2007. Atmospheric and soil drought reduce nocturnal conductance in live oaks. *Tree Physiology* **27**: 611–620.

Cheng J, Chu P, Chen D, Bai Y. 2016. Functional correlations between specific leaf area and specific root length along a regional environmental gradient in Inner Mongolia grasslands. *Functional Ecology* **30**: 985–997.

Claverie E, Meunier F, Javaux M, Sadok W. 2018. Increased contribution of wheat nocturnal transpiration to daily water use under drought. *Physiologia Plantarum* **162**: 290–300.

Claverie E, Schoppach R, Sadok W. 2016. Nighttime evaporative demand induces plasticity in leaf and root hydraulic traits. *Physiologia Plantarum* **158**: 402–413.

Cossani CM, Reynolds MP. 2013. What physiological traits should we focus on in breeding for heat tolerance? In: Alderman PD, Quilligan E, Asseng S, Ewert F, Reynolds MP, eds. *Proceedings of the workshop on modelling wheat response to high temperature*. Texcoco, Mexico: CIMMYT, 24.

Coupel-Ledru A, Lebon E, Christophe A, Gallo A, Gago P, Pantin F, Doligez A, Simonneau T. 2016. Reduced nighttime transpiration is a relevant breeding target for high water-use efficiency in grapevine. *Proceedings of the National Academy of Sciences, USA* **113**: 8963–8968.

Daley MJ, Phillips NG. 2006. Interspecific variation in nighttime transpiration and stomatal conductance in a mixed New England deciduous forest. *Tree Physiology* **26**: 411–419.

Davy R, Esau I, Chernokulsky A, Outten S, Zilitinkevich S. 2017. Diurnal asymmetry to the observed global warming. *International Journal of Climatology* **37**: 79–93.

Donovan L, Linton M, Richards J. 2001. Predawn plant water potential does not necessarily equilibrate with soil water potential under well-watered conditions. *Oecologia* **129**: 328–335.

Drake PL, De Boer HJ, Schymanski SJ, Veneklaas EJ. 2019. Two sides to every leaf: water and CO_2 transport in hypostomatous and amphistomatous leaves. *New Phytologist* **222**: 1179–1187.

Duursma RA, Blackman CJ, Lopéz R, Martin-StPaul NK, Cochard H, Medlyn BE. 2019. On the minimum leaf conductance: its role in models of plant water use, and ecological and environmental controls. *New Phytologist* **221**: 693–705.

Easlon HM, Richards JH. 2009. Photosynthesis affects following night leaf conductance in *Vicia faba*. *Plant, Cell & Environment* **32**: 58–63.

Even M, Sabo M, Meng D, Kreszies T, Schreiber L, Fricke W. 2018. Night-time transpiration in barley (*Hordeum vulgare*) facilitates respiratory carbon dioxide release and is regulated during salt stress. *Annals of Botany* **122**: 569–582.

Field CB. 1987. Leaf-age effects on stomatal conductance. In: Zeiger E, ed. *Stomatal function*. Palo Alto, CA, USA: Stanford University Press, 367.

Fischer R, Edmeades GO. 2010. Breeding and cereal yield progress. *Crop Science* **50**: S-85–S-98.

Fischer R, Rees D, Sayre K, Lu Z-M, Condon A, Saavedra AL. 1998. Wheat yield progress associated with higher stomatal conductance and photosynthetic rate, and cooler canopies. *Crop Science* **38**: 1467–1475.

Franks PJ, Beerling DJ. 2009. Maximum leaf conductance driven by CO_2 effects on stomatal size and density over geologic time. *Proceedings of the National Academy of Sciences, USA* **106**: 10343–10347.

Fricke W. 2019. Night-time transpiration-favouring growth? *Trends in Plant Science* **24**: 311–317.

García GA, Serrago RA, Dreccer MF, Miralles DJ. 2016. Post-anthesis warm nights reduce grain weight in field-grown wheat and barley. *Field Crops Research* **195**: 50–59.

Hassidim M, Dakhiya Y, Turjeman A, Hussien D, Shor E, Anidjar A, Goldberg K, Green RM. 2017. CIRCADIAN CLOCK ASSOCIATED1 (CCA1) and the circadian control of stomatal aperture. *Plant Physiology* **175**: 1864–1877.

Hein NT, Wagner D, Bheemanahalli R, Šebela D, Bustamante C, Chiluwal A, Neilsen ML, Jagadish SK. 2019. Integrating field-based heat tents and cyber-physical system technology to phenotype high night-time temperature impact on winter wheat. *Plant Methods* **15**: 41.

Howard AR, Van Iersel MW, Richards JH, Donovan LA. 2009. Night-time transpiration can decrease hydraulic redistribution. *Plant, Cell & Environment* **32**: 1060–1070.

Jones HG. 2013. *Plants and microclimate: a quantitative approach to environmental plant physiology.* Cambridge, UK: Cambridge University Press.

Kane CN, Jordan GJ, Jansen S, McAdam SA. 2020. A permeable cuticle, not open stomata, is the primary source of water loss from expanding leaves. *Frontiers in Plant Science* **11**: 774.

Kavanagh KL, Pangle R, Schotzko AD. 2007. Nocturnal transpiration causing disequilibrium between soil and stem predawn water potential in mixed conifer forests of Idaho. *Tree Physiology* **27**: 621–629.

Kerstiens G. 1996. Cuticular water permeability and its physiological significance. *Journal of Experimental Botany* **47**: 1813–1832.

Kwak MJ, Lee SH, Khaine I, Je SM, Lee TY, You HN, Lee HK, Jang JH, Kim I, Woo SY. 2017. Stomatal movements depend on interactions between external night light cue and internal signals activated by rhythmic starch turnover and abscisic acid (ABA) levels at dawn and dusk. *Acta Physiologiae Plantarum* **39**: 162.

Lawson T, Blatt M. 2014. Stomatal size, speed and responsiveness impact on photosynthesis and water use efficiency. *Plant Physiology* **164**: 1556–1570.

Lawson T, Matthews J. 2020. Guard cell metabolism and stomatal function. *Annual Review of Plant Biology* **71**: 273–302.

Li X, Ingvordsen CH, Weiss M, Rebetzke GJ, Condon AG, James RA, Richards RA. 2019. Deeper roots associated with cooler canopies, higher normalized difference vegetation index, and greater yield in three wheat populations grown on stored soil water. *Journal of Experimental Botany* **70**: 4963–4974.

Liang J, Xia J, Liu L, Wan S. 2013. Global patterns of the responses of leaf-level photosynthesis and respiration in terrestrial plants to experimental warming. *Journal of Plant Ecology* **6**: 437–447.

Lobell DB, Ortiz-Monasterio JI. 2007. Impacts of day versus night temperatures on spring wheat yields. *Agronomy Journal* **99**: 469–477.

Lobell G. 2017. Image of random root systems. Figshare. doi: 10.6084/m9.figshare.4684924.v2.

Lombardozzi DL, Zeppel MJ, Fisher RA, Tawfik A. 2017. Representing nighttime and minimum conductance in CLM4. 5: global hydrology and carbon sensitivity analysis using observational constraints. *Geoscientific Model Development* **10**: 321–331.

Lu Z, Percy RG, Qualset CO, Zeiger E. 1998. Stomatal conductance predicts yields in irrigated Pima cotton and bread wheat grown at high temperatures. *Journal of Experimental Botany* **49**(Special Issue): 453–460.

Marks CO, Lechowicz MJ. 2007. The ecological and functional correlates of nocturnal transpiration. *Tree Physiology* **27**: 577–584.

Martre P, Reynolds MP, Asseng S, Ewert F, Alderman PD, Cammarano D, Maiorano A, Ruane AC, Aggarwal PK, Anothai J. 2017. The International Heat Stress Genotype Experiment for modeling wheat response to heat: field experiments and AgMIP-wheat multi-model simulations. *Open Data Journal for Agricultural Research* **3**: 23–28.

Matyssek R, Günthardt-Goerg MS, Maurer S, Keller T. 1995. Nighttime exposure to ozone reduces whole-plant production in *Betula pendula*. *Tree Physiology* **15**: 159–165.

McAusland L, Vialet-Chabrand S, Davey P, Baker NR, Brendel O, Lawson T. 2016. Effects of kinetics of light-induced stomatal responses on photosynthesis and water-use efficiency. *New Phytologist* **211**: 1209–1220.

McAusland L, Vialet-Chabrand S, Jauregui I, Burridge A, Hubbart-Edwards S, Fryer MJ, King IP, King J, Pyke K, Edwards KJ *et al.* 2020. Variation in key leaf photosynthetic traits across wheat wild relatives is accession-dependent not species-dependent. *New Phytologist* **228**: 1767–1780.

Moore CE, Meacham-Hensold K, Lemonnier P, Slattery RA, Benjamin C, Bernacchi CJ, Lawson T, Cavanagh AP. 2021. The effect of increasing temperature on crop photosynthesis: from enzymes to ecosystems. *Journal of Experimental Botany* **72**: 2822–2844.

Mott KA, Gibson AC, O'Leary JW. 1982. The adaptive significance of amphistomatic leaves. *Plant, Cell & Environment* **5**: 455–460.

O'Leary BM, Lee CP, Atkin OK, Cheng R, Brown TB, Millar AH. 2017. Variation in leaf respiration rates at night correlates with carbohydrate and amino acid supply. *Plant Physiology* **174**: 2261–2273.

Parlange J-Y, Waggoner PE. 1970. Stomatal dimensions and resistance to diffusion. *Plant Physiology* **46**: 337–342.

Pathare VS, Koteyeva N, Cousins AB. 2020. Increased adaxial stomatal density is associated with greater mesophyll surface area exposed to intercellular air spaces and mesophyll conductance in diverse C4 grasses. *New Phytologist* **225**: 169–182.

Pearcy RW, Schulze ED, Zimmermann R. 2000. Measurement of transpiration and leaf conductance. In: Pearcy RW, Ehleringer JR, Mooney HA, Rundel PW, eds. *Plant physiological ecology.* Dordrecht, the Netherlands: Springer, 137–160.

Peng S, Huang J, Sheehy JE, Laza RC, Visperas RM, Zhong X, Centeno GS, Khush GS, Cassman KG. 2004. Rice yields decline with higher night temperature from global warming. *Proceedings of the National Academy of Sciences, USA* **101**: 9971–9975.

Phillips NG, Lewis JD, Logan BA, Tissue DT. 2010. Inter-and intra-specific variation in nocturnal water transport in *Eucalyptus*. *Tree Physiology* **30**: 586–596.

Posch BC, Kariyawasam BC, Bramley H, Coast O, Richards RA, Reynolds MP, Trethowan R, Atkin OK. 2019. Exploring high temperature responses of photosynthesis and respiration to improve heat tolerance in wheat. *Journal of Experimental Botany* **70**: 5051–5069.

Rasband WS. 1997–2018. *ImageJ*. Bethesda, MD, USA: U. S. National Institutes of Health. [WWW document] URL https://imagej.nih.gov/ij/ [accessed 1 Feburary 2020].

Rawson H, Clarke J. 1988. Nocturnal transpiration in wheat. *Functional Plant Biology* **15**: 397–406.

Resco de Dios V, Chowdhury FI, Granda E, Yao Y, Tissue DT. 2019. Assessing the potential functions of nocturnal stomatal conductance in C3 and C4 plants. *New Phytologist* **223**: 1696–1706.

Resco de Dios V, Díaz-Sierra R, Goulden ML, Barton CV, Boer MM, Gessler A, Ferrio JP, Pfautsch S, Tissue DT. 2013a. Woody clockworks: circadian regulation of night-time water use in *Eucalyptus globulus*. *New Phytologist* **200**: 743–752.

Resco de Dios V, Loik ME, Smith R, Aspinwall MJ, Tissue DT. 2016. Genetic variation in circadian regulation of nocturnal stomatal conductance enhances carbon assimilation and growth. *Plant, Cell & Environment* **39**: 3–11.

Resco de Dios V, Roy J, Ferrio JP, Alday JG, Landais D, Milcu A, Gessler A. 2015. Processes driving nocturnal transpiration and implications for estimating land evapotranspiration. *Scientific Reports* **5**: 10975.

Resco de Dios V, Turnbull MH, Barbour MM, Ontedhu J, Ghannoum O, Tissue DT. 2013b. Soil phosphorous and endogenous rhythms exert a larger impact than CO_2 or temperature on nocturnal stomatal conductance in *Eucalyptus tereticornis*. *Tree Physiology* **33**: 1206–1215.

Rogiers SY, Clarke SJ. 2013. Nocturnal and daytime stomatal conductance respond to root-zone temperature in 'Shiraz' grapevines. *Annals of Botany* **111**: 433–444.

Sack L, Cowan P, Jaikumar N, Holbrook N. 2003. The 'hydrology' of leaves: co-ordination of structure and function in temperate woody species. *Plant, Cell & Environment* **26**: 1343–1356.

Sadok W, Jagadish SK. 2020. The hidden costs of nighttime warming on yields. *Trends in Plant Science* **25**: 644–651.

Schoppach R, Claverie E, Sadok W. 2014. Genotype-dependent influence of night-time vapour pressure deficit on night-time transpiration and daytime gas exchange in wheat. *Functional Plant Biology* **41**: 963–971.

Schoppach R, Sinclair TR, Sadok W. 2020. Sleep tight and wake-up early: nocturnal transpiration traits to increase wheat drought tolerance in a Mediterranean environment. *Functional Plant Biology* **47**: 1117–1127.

Screen JA. 2014. Arctic amplification decreases temperature variance in northern mid-to high-latitudes. *Nature Climate Change* **4**: 577–582.

Sillmann J, Kharin VV, Zwiers F, Zhang X, Bronaugh D. 2013. Climate extremes indices in the CMIP5 multimodel ensemble: Part 2. Future climate projections. *Journal of Geophysical Research: Atmospheres* **118**: 2473–2493.

Slafer G, Rawson H. 1995. Base and optimum temperatures vary with genotype and stage of development in wheat. *Plant, Cell & Environment* **18**: 671–679.

Snyder K, Richards J, Donovan L. 2003. Night-time conductance in C3 and C4 species: do plants lose water at night? *Journal of Experimental Botany* **54**: 861–865.

Tamang BG, Sadok W. 2018. Nightly business: links between daytime canopy conductance, nocturnal transpiration and its circadian control illuminate physiological trade-offs in maize. *Environmental and Experimental Botany* **148**: 192–202.

Thomas J, Prasad P. 2003. Plants and the environment; global warming effects. In: Thomas B, Murray BG, Murphy DJ, eds. *Encylopedia of applied plant sciences*. Oxford, UK: Academic Press, 297.

Tricker PJ, ElHabti A, Schmidt J, Fleury D. 2018. The physiological and genetic basis of combined drought and heat tolerance in wheat. *Journal of Experimental Botany* **69**: 3195–3210.

Wachendorf M, Küppers M. 2017. The effect of initial stomatal opening on the dynamics of biochemical and overall photosynthetic induction. *Trees* **31**: 981–995.

Wang H, Atkin OK, Keenan TF, Smith NG, Wright IJ, Bloomfield KJ, Kattge J, Reich PB, Prentice IC. 2020. Acclimation of leaf respiration consistent with optimal photosynthetic capacity. *Global Change Biology* **26**: 2573–2583.

Wang Y, Anderegg WR, Venturas MD, Trugman AT, Yu K, Frankenberg C. 2021. Optimization theory explains nighttime stomatal responses. *New Phytologist* **230**: 1550–1561.

Wasson AP, Richards R, Chatrath R, Misra S, Prasad SS, Rebetzke G, Kirkegaard J, Christopher J, Watt M. 2012. Traits and selection strategies to improve root systems and water uptake in water-limited wheat crops. *Journal of Experimental Botany* **63**: 3485–3498.

Wei T, Simko V. 2016. *corrplot: visualization of a correlation matrix.0.84.* [WWW document] URL https://cran.r-project.org/web/packages/corrplot/corrplot.pdf [accessed 30 January 2020].

Welch JR, Vincent JR, Auffhammer M, Moya PF, Dobermann A, Dawe D. 2010. Rice yields in tropical/subtropical Asia exhibit large but opposing sensitivities to minimum and maximum temperatures. *Proceedings of the National Academy of Sciences, USA* **107**: 14562–14567.

Yu K, Goldsmith GR, Wang Y, Anderegg WR. 2019. Phylogenetic and biogeographic controls of plant nighttime stomatal conductance. *New Phytologist* **222**: 1778–1788.

Zadoks JC, Chang TT, Konzak CF. 1974. A decimal code for the growth stages of cereals. *Weed Research* **14**: 415–421.

Zeppel MJ, Lewis JD, Chaszar B, Smith RA, Medlyn BE, Huxman TE, Tissue DT. 2012. Nocturnal stomatal conductance responses to rising [CO_2], temperature and drought. *New Phytologist* **193**: 929–938.

Supporting Information

Additional Supporting Information may be found online in the Supporting Information section at the end of the article.

Fig. S1 The diurnal responses of photosynthetic CO_2 assimilation (A) in five biological replicates of modern genotype *T. aestivum* 'Paragon' and wild relative *T. urartu* 1010001.

Fig. S2 Leaf-surface-specific differences in g_{sn} pre-flag leaf emergence in eight modern *T. aestivum* genotypes.

Fig. S3 The genotype-specific responses of stomatal conductance pre-dawn (g_{sn}), 4 h post dawn (g_s), nocturnal respiration (R_d) and CO_2 assimilation (A) in six modern spring wheat genotypes and two Watkins landraces.

Fig. S4 The relationship between net respiratory CO_2 release (R_d) and net photosynthetic CO_2 assimilation (A) in six modern spring wheat genotypes and two Watkins landraces.

Fig. S5 The growth-stage specific responses of pre-dawn respiration (R_d) and 4 h post-dawn rates of CO_2 assimilation (A) in six modern spring wheat genotypes and two Watkins landraces.

Fig. S6 A correlation matrix of all characteristics measured either compared as a mean of the data across the lifespan of the plant or comparing individual growth stages.

Fig. S7 The intrinsic water-use efficiency (W_i) of six modern genotypes and two Watkins landraces. Data are separated to reflect genotype and growth-stage specific differences.

Fig. S8 The stomata dimensions of pore length, guard cell with, pore area and, incorporating stomatal density, an estimation of anatomical maximum conductance (g_{smax}) of six modern genotypes and two Watkins landrace genotypes.

Fig. S9 A graphical representation of the phenology of six modern spring wheat cultivars and two Watkins landraces.

Fig. S10 The harvest traits of six modern genotypes and two Watkins landrace genotypes.

Please note: Wiley Blackwell are not responsible for the content or functionality of any Supporting Information supplied by the authors. Any queries (other than missing material) should be directed to the *New Phytologist* Central Office.